JAHRBUCH DER GEOLOGISCHEN BUNDESANSTALT

Jb. Geol. B.-A. | ISSN 0016-7800 | Band 149 | Heft 1 | S. 7–21 | Wien, Juli 2009

Paleokarst Phenomena and Peritidal Beds in the Cyclic Dachstein Limestone on the Dachstein Plateau (Northern Calcareous Alps, Upper Austria)

JÁNOS HAAS*), OLGA PIROS**), ÁGNES GÖRÖG***) & HARALD LOBITZER****)

14 Text-Figures, 4 Plates

Oberösterreich
Trias
Ladin
Dachsteinkalk
Paläokarst

Contents

Paläokarst-Phänomene und peritidale Ablagerungen im gebankten Dachstein-Kalk auf dem Dachsteinplateau (Nördliche Kalkalpen, Oberösterreich)

Zusammenfassung

Es wurden Aufschlüsse der norischen zyklischen Dachsteinkalke auf dem Dachsteinplateau, Nördliche Kalkalpen, Österreich, untersucht. Der Schwerpunkt lag auf den Zyklus-Intervallen. Ausgeprägte Diskordanzen mit Charakteristika von subärischer Erosion, Verwitterung und Karstlösung auf und unter den alten Landoberflächen werden gezeigt. In manchen Fällen konnten nur schwache Spuren subaerischer Erosion beobachtet werden, sichtbar in ausgeprägteren Lösungserscheinungen und meteorisch-diagenetischer Umwandlung auf den Schichtflächen. Pedogenese und meteorische Diagenese wirkten sich auf subtidale und peritidale Karbonatablagerungen während der Emersionsperioden aus. Typisch ist die Bildung von Caliche-Krusten auf den trockengefallenen Oberflächen, auch aufgearbeitete Kalkkrusten sowie Gerölle von geschwärzten Karbonaten kommen vor. Ostrakoden führende Gezeitentümpel-Sedimente finden sich in den Karstsenken und Hohlräumen. Diese Belege für subaerische Freilegung zwischen den subtidalen und peritidalen Ablagerungen unterstützen die These einer allozyklischen Steuerung der Lofer-Zyklen.

Abstract

Exposures of the Norian cyclic Dachstein Limestones were studied on the Dachstein plateau, Northern Calcareous Alps, Austria, focusing on the cycle boundary intervals. Pronounced disconformities showing characteristic features of subaerial erosion, weathering and karstic solution on and below the paleosurfaces were pointed out, but in some cases only subtle traces of the subaerial exposure, that has manifested itself in the more pronounced solution features, and meteoric diagenetic alterations below the bedding planes could be observed. Pedogenesis and meteoric diagenesis affected the subtidal-peritidal carbonate deposits during the emersion periods. Calcretes forming on the top of the truncated bed sets are typical. Rip-up chips of calcretes, pebbles of blackened carbonates are also common. Ostracode-bearing tidal-flat pool sediments typically occur in the karstic depressions and cavities. Evidences for subaerial exposures between the subtidal-peritidal deposits support the allocyclic control of the Lofer cyclicity.

*) JÁNOS HAAS, Geological, Geophysical and Space Science Research group of the Hungarian Academy of Sciences, Eötvös Loránd University, Pázmány sétány 1/C, H 1117 Budapest, Hungary.
**) OLGA PIROS, Hungarian Geological Institute, Stefánia út 14, H 1143 Budapest, Hungary.
***) ÁGNES GÖRÖG, Paleontological Department, Eötvös Loránd University, Pázmány sétány 1/C, H 1117 Budapest, Hungary.
****) HARALD LOBITZER, Lindaustraße 3, A 4820 Bad Ischl, Austria.

1. Introduction

The Upper Triassic Dachstein Limestone plays an outstanding role in the building up of the Northern Calcareous Alps. It was formed by a tropical shallow marine carbonate factory of an extremely large carbonate platform system continuously developed during a period of about 20 Ma. Moreover, the extension of the Dachstein-type platform carbonates far exceeds the region of the Eastern Alps; they are known all along the margin of the Late Triassic Tethys Ocean.

SIMONY (1847) named the thick bedded, *Megalodus*-bearing limestone formation "Dachsteinkalk" after the Dachstein Range. SUESS (1888) described red marl interlayers in the Dachstein Limestone and interpreted them as results of periodical subaerial exposure.

SANDER (1936) first recognised metre-scale sedimentary cycles in the Dachstein Limestone, terming this cyclic facies as Lofer facies because of its excellent exposure in the Loferer Steinberge, and attributed the cyclicity to sea level changes. SCHWARZACHER (1948, 1954) recognised a higher order organisation of the cycles i.e. the basic cycles are organised to bundles, in a ratio 5:1, suggesting precession – short eccentricity ratio. Based on studies in the Loferer Steinberge, Steinernes Meer and Dachstein, FISCHER (1964) presented a detailed description of the facies characteristics of the members of the cycles ("Lofer cyclothems") defining an upward-deepening facies trend and proposed orbital control of the cyclicity. He characterised and interpreted the typical Lofer cycle as follows:

- a disconformity at the base;
- member A – a basal argillaceous member (red or green) representing reworked residue of weathered material;
- member B – intertidal member of loferites with algal mats and abundant desiccation features;
- member C – subtidal megalodont limestone.

HAAS (1982, 1991, 1994) modified the basic pattern of the Lofer cycles, proposing a symmetrical ideal cycle. GOLDHAMMER et al. (1990) and SATTERLEY (1996a) reinterpreted the ideal Lofer cycle as shallowing upward. SATTERLEY (1996a,b) and ENOS & SAMANKASSOU (1998) stressed the lack of evidence for subaerial exposure at the cycle boundaries and assumed allocyclicity as the predominant control. In contrast, studies of HAAS et al. (2007) in the Krippenstein area provided a number of evidences for subaerial exposure and related karstification and peculiar sediment deposition. However, the evaluation of the characteristic features and main control for Lofer cyclicity is still subject to debates. Main aim of this paper is to present further evidences for periodical subaerial exposures that punctuated the carbonate platform evolution and features formed in the course of the related pedogenic and meteoric diagenetic processes, based on studies in the type locality of the Dachstein Limestone.

2. Geological Setting

The area studied is located in the Dachstein mountain range, Northern Calcareous Alps, Austria (Text-Fig. 1a). The Northern Calcareous Alps are an allochthonous fold-and-thrust belt. Alpine history of this unit initiated in the Late Permian – Early Triassic with deposition of evaporites and terrestrial red beds. In the Middle to Late Triassic interval, shallow marine carbonates deposited in this area that was a segment of the passive margin of the Tethys Ocean. In the Norian–Rhaetian, large rimmed platforms developed where thick carbonate sequences were accumulated keeping pace with the subsidence (Hauptdolomit – Dachstein Limestone). Progressing rifting and facies differentiation initiated in the Early Jurassic which was followed by a general deepening and widespread deposition of pelagic facies in the Middle and Late Jurassic. According to recent studies, emplacement of slabs of basin and platform facies started in the Middle Jurassic (GAWLICK & FRISCH, 2003). Major thrusting phases occurred in the Early and middle Cretaceous and the Early Tertiary (MANDL, 2000; FRANK & SCHLAGER, 2006).

The Dachstein Mountains comprise a stratigraphic succession starting with the Upper Permian Haselgebirge that contains the famous salt deposits in the surroundings of Hallstatt. Type localities of well-known Triassic lithostratigraphic units and facies types, e.g. the basinal Hallstatt Limestone and the platform carbonates of the Dachstein Limestone, occur in this area. The Dachstein plateau is made up of Norian–Rhaetian cyclic Dachstein Limestone

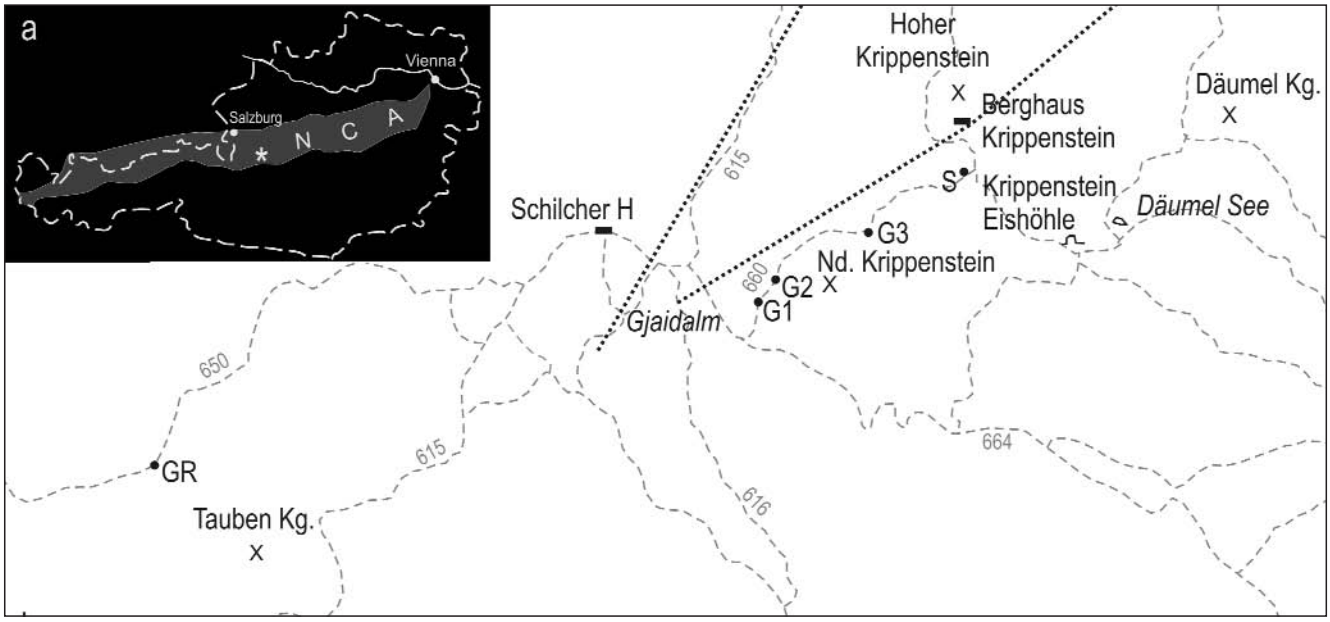

Text-Fig. 1.
a) Geologic setting of the study area.
b) Location of the studied sections and occurrences on the Dachstein Plateau.
G 1–3 = sampling point along the ski-trail between Gjaidalm and Krippenstein Schutzhaus; S = section at Krippenstein Schutzhaus; GR = Gretl-Rast section.

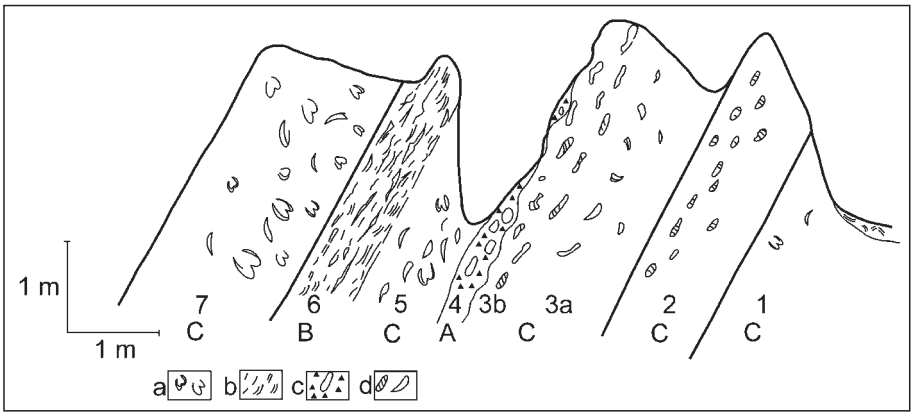

Text-Fig. 2.
Facies succession in the Gretl-Rast section.
a) Megalodonts, b) Bird's eyes and sheet cracks, c) Lithoclasts and black pebbles, d) Solution cavities,with geopetal filling.

characterised by alternation of peritidal and inner platform lagoon facies. Reef facies of the Dachstein Limestone is exposed westward, in the neighbourhood of Gosau Lake (Gosaukamm [FLÜGEL, 1981]). The Dachstein Limestone is directly overlain by the Lower Jurassic Hierlatz Limestone or the Middle Jurassic Klauskalk. Classic localities of these formations are located in the Dachstein Mountains, which are also rimmed in the northwest by the type area of the Upper Cretaceous to Palaeogene Gosau Group.

3. Studied Occurrences

The studied occurrences are located in the central part of the Dachstein plateau (Text-Fig. 1b). In accordance with the aim of the work, exposures of the cycle boundary intervals i. e. the disconformity surfaces, the altered topmost part of the cycles and the usually variegated basal layers of the overlying cycles were selected for detailed observations and sampling. In the Gretl-Rast section a bed set is exposed along a protected trail, and widening of this trail improved the exposure conditions just at the critical part of the succession. A newly made ski trail between Gjaidalm and Krippenstein provided fresh exposures of several cycles. The best one is located below the Krippenstein Schutzhaus which exposed a 12 m thick continuous succession described in detail by HAAS et al. (2007). However, there are good although less continuous exposures along the ski trail, which were also documented and sampled. Results of the microfacies studies of these occurrences are also presented in this paper.

3.1. Gretl-Rast Section

An excellent example for a karstified cycle termination and peritidal deposits at the base of an overlying cycle is exposed beside the protected trail between Oberfeld and Wiesberghaus (N 47° 30' 55.5", E 13° 38' 55.6"). The studied section is presented in Text-Fig. 2.

Light brownish grey limestone (Bed 1) containing several Megalodonts is exposed in the lowermost part of the studied interval. It has a bioclastic wackestone texture with micropeloidal microsparitic matrix. The bioclasts are molds of bivalves, gastropods and foraminifera (*Auloconus permodiscoides* (OBERHAUSER), *Glomospira regularis* LIPINA [Plate 1, Figs. 1,2]). In some irregular patches, tiny solution pores are visible among the grains (Plate 2/1). Solution voids formed by enlargement of the moldic pores are also common. In the larger pores geopetal fill occurs.

This bed was formed under shallow subtidal conditions, on the low to medium energy inner platform (C facies). The carbonate sediment was subject to meteoric diagenesis, subsequently.

The next bed (Bed 2) is macroscopically similar to the one previously described, but it contains small solution cavities and dissolved megalodonts filled by dark red micrite. Peloidal wackestone-grainstone was the original texture but there are a lot of cm sized solution cavities with geopetal fill (Plate 2/2). In the sample studied, the volume of the cavity fill exceeds the volume of the host rock. The internal sediment in the cavity fill is patchy micrite-microsparite in which thin-shelled ostracodes are common. A few foraminifera (*Agathammina austroalpina* KRISTAN-TOLLMANN & TOLLMANN, *Diplotremina*? sp.) occur too (Plate. 1/3). The remnant parts of the cavities are filled by sparry calcite.

The low energy subtidal zone of the inner platform was the depositional area (C facies). The more or less consolidated deposit was subject to intense karstic solution in the course of the subsequent subaerial exposure. The cavities were filled by ostracode-bearing mud probably of tidal flat pool origin, and meteoric cement subsequently.

The overlying bed (Bed 3) is somewhat darker than the previous one, but macroscopically similar. Its texture is packstone, containing bioclasts (mollusc fragments and foraminifera) and oomolds. Foraminifers are mostly strongly recrystallized Involutinidae; few specimens of *Frondicularia woodwardi* HOWCHIN, *Agathammina austroalpina, Ophthalmidium* ssp. and *Trochammina* also occur (Plate 1/4). There are a few intraclasts (Plate 2/3). Solution pores formed by enlargement of moldic pores are common. They usually have geopetal fills. In some cases microbial encrustation was observed on the upper wall of the cavity i.e. above the sparry calcite of the geopetal fill (Plate 2/4).

In the uppermost 20–50 cm of this bed there are a number of cm sized karstic solution cavities that are filled by red argillaceous micrite. Under the microscope, thin-

Text-Fig. 3.
Solution cavities filled by red argillaceous limestone in the upper part of Bed 3, below the disconformity surface.
Gretl-Rast section.

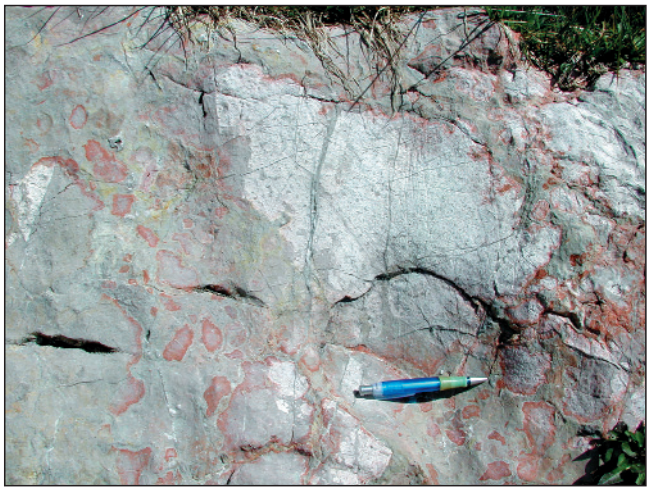

Text-Fig. 4.
Rip-ups of stromatolites in greenish argillaceous limestone in Bed 4.
Gretl-Rast section.

shelled ostracods were found in the micritic fill. In some cases secondary solution pores with sparry calcite occur within the micritic cavity fill. Foraminifera are common in the host rock. Involutinidae (*Angulodiscus communis* KRISTAN, *Aulotortus* cf. *sinuosus* WEYNSCHENK), Nodosariidae (*Frondicularia woodwardi, Nodosaria* sp., *Dentalina* sp.), *Agathammina austroalpina, Miliolipora cuvillieri* BRÖNNIMANN & ZANINETTI, *Diplotremina*? sp., *Glomospira sp., Trochammina* sp., *Gaudryina triadica* KRISTAN-TOLLMANN, *Earlandia* sp. and *Earlandinita* sp. were found (Plate 1/5–11).

There is an uneven erosional surface above Bed 3 that can be interpreted as a subaerial exposure horizon. The 10–15 cm deep karstic depressions of the bedding plane are filled by greenish-ochre clayey micrite (Text-Fig. 3). The disconformity surface is overlain by reddish-greenish argillaceous limestone, containing rip-ups of stromatolites, 1–20 cm in size (Text-Fig. 5, 6), and black pebbles, 0.5–5 cm in size (Bed 4 – A facies).

In a sample taken from the matrix a network of irregular cracks and circum-granular cracks filled by microspar (Plate 2/5) and small microsparite nodules and elongated solution cavities, usually with geopetal fill (Plate 1/6) were observed, which are characteristic features of the alpha calcretes (WRIGHT, 1990). A few cm sized megalodont fragments, detritus of dasycladaceean algae (*Teutloporella* cf. *peniculiformis*) and a number of microsparitized foraminifera (*Angulodicus friedli* (KRISTAN-TOLLMANN)) are the most common, *A. communis, A. gasche*i KOEHN-ZANINETTI & BRÖNNIMANN, *A.* cf. *minutus* (KOEHN-ZANINETTI), *A.* cf. *tenuis* KRISTAN, *Galeanella panticae* ZANINETTI & BRÖNNIMANN and very few Nodosariidae were found (Plate 1/12–20). The large Involutinidae are often broken or/and bioeroded.

In another sample 0.8 to 2.0 cm sized lithoclasts were visible in a patchy micrite-microsparite matrix. Thin-shelled ostracodes are common in the matrix. There are a few mm sized bioclasts (fragments of echinoderms, megalodonts, dasycladaceean algae), and various lithoclasts (Plate 3/1). The following clast types were observed:

a) blackened mudstone with a few thin-shelled ostracods, micritized foraminifera, gastropods, and microsparite patches; there is a thin iron-oxide coating on the clast (Plate 3/1),
b) blackened wackestone with fenestral pores; this clast is also encrusted by iron-oxide,
c) red micrite with solution cavities and bioeroded bioclasts (fragments of megalodonts, dasycladaceean algae, micritized foraminifera) and small blackened intraclasts.

The features of Bed 4 imply subaerial weathering, pedogenesis in a tidal flat setting, that is manifested itself in blackening, formation of clasts and lumps with iron-oxide coating, brecciation. The coarse- to fine-grained weathering material was subject to short-distance multiple reworking and redeposition in the tidal-flat pools and this deposit was also affected by incipient pedogenesis leading to the formation of a calcrete fabric.

The red argillaceous layer is overlain by a light greyish brown limestone bed (Bed 5) containing larger fragments of megalodonts. It has a clotted peloidal micritic-microsparitic texture. A great number of thin-shelled ostracode valves occur both in the micritic and microsparitic patches (Plate 3/3). Dissolution pores and small cavities with drusy calcite infilling are common.

Textural features of this bed suggest microbially induced carbonate formation, but no trace of desiccation was observed. A tidal flat pool or a protected lagoon may have been the depositional environment. Abundance of ostracods supports the former option (Plate 2/21–22). The megalodont fragments and the few foraminifera (*Angulodiscus* spp., *Semiinvolutina* sp., *Trochammina* sp. and Oberhauserellidae sp.) are certainly reworked, probably storm transported.

The next white loferitic interval (Bed 6) continuously progresses from the previously described bed, there is no bed-

Text-Fig. 5.
Rip-ups of stromatolites in greenish-reddish argillaceous limestone in Bed 4.
Gretl-Rast section.

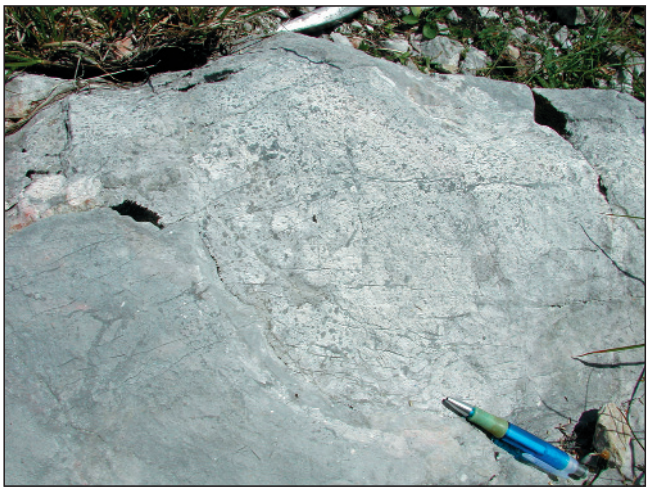

Text-Fig. 6.
Loferitic limestone with bird's eye pores and sheet cracks in Bed 6.
Gretl-Rast section.

ding plane between them. It is typified by mm sized bird's eye voids and sheet cracks, 2–5 cm in length (Fig. 6).

It contains foraminifera (*Turrispirillina minima* PANTIČ, and *Angulodiscus friedli* are the most frequent, moreover *Aulotortus sinuosus* and *Turrispirillina* sp. occur; Plate 1/23–26), suggesting deposition of shallow marine carbonate mud. On the other hand, it has a calcrete-type micritic-microsparitic texture. The micritic patches are usually stained to brown and they contain fenestral pores. There are cm sized irregular patches that may have been solution cavities, some of them formed in the place of roots (Plate 3/4, 5). They often have geopetal fill, but in some cases the outer part of the cavities are filled by micrite whereas their central part is filled by sparite, implying root cast origin of these objects. The cavity fill is micrite or microsparite-calcisilt, with a lot of ostracode valves, locally. The observed features suggest pedogenic alteration of the originally deposited carbonate mud due to a sea-level drop that resulted in temporal subaerial conditions. Tidal flat pools may have been the source of the ostracode-bearing cavity fill mud.

Above a sharp boundary the calcrete bed is followed by a thick limestone bed, abundant in megalodonts (Bed 7). It has a peloidal bioclastic packstone-grainstone texture, containing cm sized fragments of chaetetid calcisponges (Plate 3/6), some foraminifera (*Diplotremina* sp., *Miliolipora cuvillieri*, *Glomospirella* sp., *Angulodiscus* sp.) (Plate 2/27–28) and Tubiphytes-type nodules and encrustations. It was formed under subtidal conditions (C facies).

Summing up, the section studied is made up by peritidal and subtidal facies characteristic elements of the Lofer cycles. In spite of excellent exposure conditions, recognition of the basic cycles is not plausible. The macroscopic observations are not satisfactory, microfacies studies are needed to establish the real facies succession.

For example, evaluation of traces of meteoric diagenesis in Bed 2 is rather problematic. Taking into consideration that solution cavities in this bed are much more common than those in the overlying bed, the possibility of a short subaerial interval between deposition of Bed 2 and 3 cannot be excluded.

The cycle termination above Bed 3 is constrained by a well developed disconformity surface and evidences for karstification. The overlying beds (4, 5, 6) are probably tidal flat deposits, although Bed 5 formed in a permanently inundated environment, that was followed by a pedogenic period, represented by Bed 6. However, these facies changes are likely results of autocyclic processes, rather than sea-level changes. Abrupt appearance of subtidal facies in Bed 7 clearly indicates sea-level controlled transgression.

Based on the frequence of *Angulodiscus friedli* and *Agathammina austroalpina*, and the co-occurrence of *Miliolipora cuvillieri, Turrispirillina minima, Angulodiscus communis* and *Angulodiscus tenuis* (KRISTAN, 1957; KRISTAN-TOLLMANN, 1962; BRÖNNIMANN et al., 1972; PANTIČ, 1967) and the lack of *Triasina hantkeni*, the age of these rocks are Norian, probably Late Norian.

3.2. Outcrops along the Ski Trail between Gjaidalm and Krippenstein

A newly made ski trail exposed a significant interval of the cyclic Dachstein Limestone. The best exposure along this trail was encountered below the Krippenstein Schutzhaus where a 12 m thick segment of the formation could be studied (Text-Fig. 7). In the measured section ABCB', BCB', ABC, C facies stacking patterns were recognised. A detailed description of the succession, including the microfacies characteristics of the beds is presented by HAAS et al. (2007). Accordingly those features are highlighted here, which are in close connection with the topic of this paper.

The exposed section begins with a thick limestone bed (C facies). Its upper bedding plane is an uneven disconformity surface (Text-Fig. 8). Cracks, pockets and cavities filled by red and grey mudstone occur in the uppermost 30 cm of the bed. Small moldic pores filled by sparry calcite are common. The larger amalgamated pores and cavity networks are filled totally or partially by carbonate silt – microsparite. Ostracodes are rarely present in the lower part of the geopetal pore fills.

The disconformity is covered by 1–2 cm thick red argillaceous mudstone (facies A) that is succeeded by white, dolomitised mudstone with fenestral pores and mm-wide desiccation cracks (loferite – facies B) in a thickness of 17 cm and then by a 20 cm thick crinkle stromatolite layer. It is followed by light grey limestone (facies C) that is succeeded by 5 to 10 cm of white, laminated dolomitised mudstone with desiccation cracks (facies B). An uneven disconformity surface ends the cycle that is covered by 2–5 cm red, argillaceous mudstone (facies A). It is followed by an 1 m thick stromatolitic-loferitic interval (facies B).

There is a sharp boundary between the upper loferitic bed and the overlying 2.5 m thick light grey wackestone bed (facies C). It is bound by an uneven disconformity surface that is covered by 2–10 cm of red or greenish grey mudstone (facies A) containing a number of ostracodes (Fig. 9). This basal layer is overlain by grey mudstone that is succeeded by a gastropod-rich horizon and then a yellowish-white dolomitic mudstone interval with shrinkage cracks. A slightly uneven

Text-Fig. 7.
Section along the ski-trail below the Krippenstein Schutzhaus 3658.

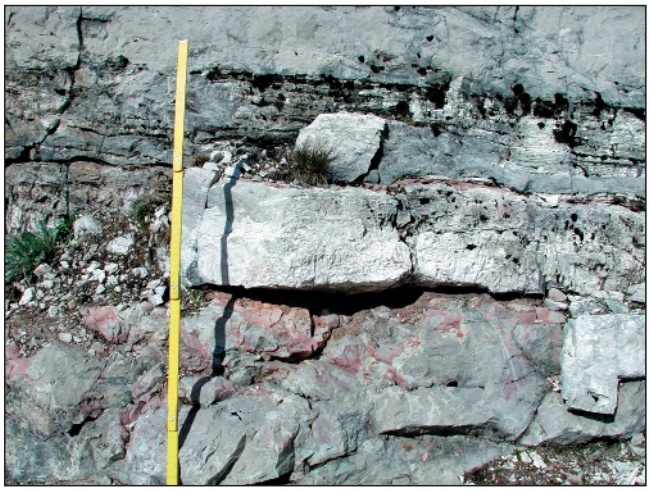

Text-Fig. 8.
Karstified disconformity surface and overlying peritidal layers in the lower part of the section below the Krippenstein Schutzhaus 3665.

disconformity surface closes this cycle that is covered by greenish grey argillaceous mudstone 1–4 cm in thickness. Solution of a sample taken from this layer yielded well-preserved ostracodes in a relatively large number similar to those described by KOZUR as *Lutkevichinella* aff. *grammi* KOZUR, 1972 n. sp. from the Rhaetian Dachstein Limestone in the Transdanubian Range, Hungary (HAAS et al., 2007).

The ostracode-bearing greenish mudstone grades upward into yellow mudstone with scattered fenestral pores and small gastropods. It is succeeded by stromatolite with shrinkage cracks and cm sized cavities. The next 1.8 m thick bed is made up of bioclastic, peloidal grainstone (C facies). It is bounded by an uneven disconformity surface showing microkarstic features. The solution pockets are filled by red mudstone. A bed showing similar facies characteristics and thickness as the underlying one (facies C) overlies this surface.

Along the ski trail several other newly exposed segments of the Dachstein Limestone succession were found. Although a continuous section could not be measured, the exposures permitted detailed observation, documentation and sampling of the boundary interval (top and base) of many cycles. The locations of the studied intervals are shown in Text-Fig. 1b.

Very pronounced disconformity surfaces and definite karstic features were observed at the base of the cycles.

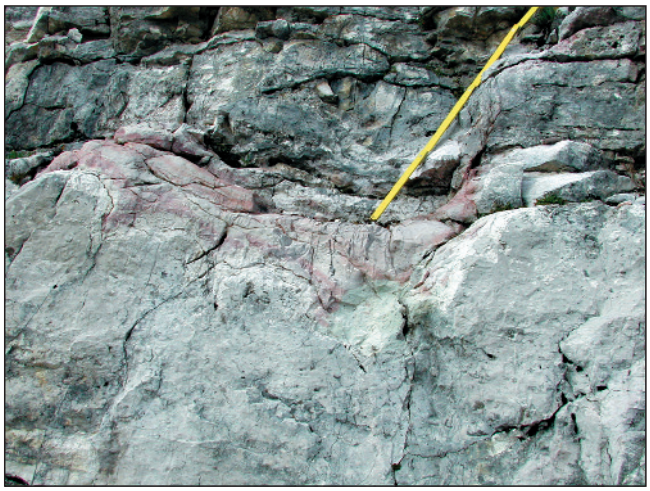

Text-Fig. 9.
Karstified boundary of a cycle in the upper part of the section below the Krippenstein Schutzhaus 3672.

Text-Fig. 10.
Network of solution pipes and cavities filled by red mudstone-wackestone. Ski trail between Gjaidalm and Krippenstein (G 2).

Below the disconformity surface, in a 0.5 to 1 m thick interval, a network of solution pipes and cavities filled by red mudstone is visible (Text-Fig. 10). Above the disconformity, a 5 to 10 cm red mudstone layer occurs that commonly contains blackened and non-blackened lithoclasts

Text-Fig. 11.
Brown and black clasts in a tan mudstone matrix with solution cavities filled by sparry calcite.

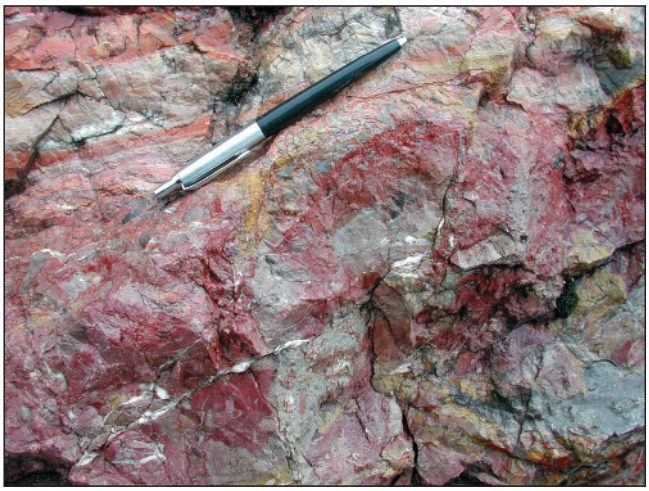

Text-Fig. 12.
Small blackened and non-blackened clasts in red mudstone cavity fill. Ski trail between Gjaidalm and Krippenstein (G 2).

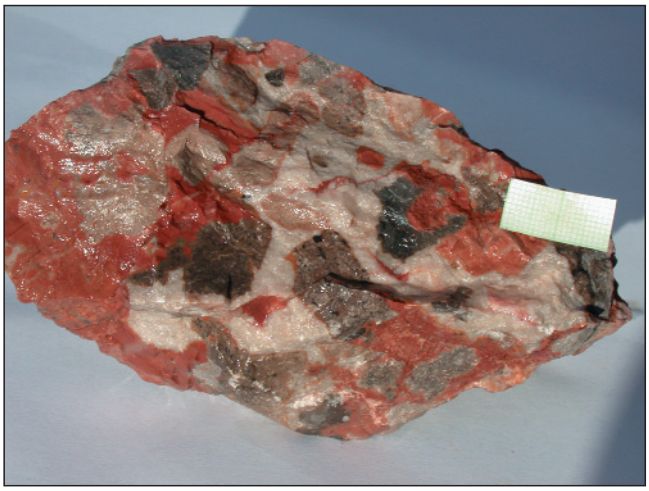

Text-Fig. 13.
Dark brown and black clasts in red mudstone and white sparitic cavity fill. Ski trail between Gjaidalm and Krippenstein (G 3).

(A facies) (Text-Fig. 11). The same material or locally calcite cement fills the solution pipes, pockets and cavities (Text-Figs. 12, 13).

Samples collected from 3 occurrences of the A facies (Gj1, 2, 3 on Text-Fig. 1A), showed very similar microfacies characteristics. The typical texture is lithoclastic wackestone. The matrix is argillaceous micrite-microsparite mudstone to wackestone, containing thin-shelled ostracodes in varying abundance, few foraminifera (*Agathammina austroalpina, Glomospirella amplificata* KRISTAN-TOLLMANN, *Pilammina densa* PANTIČ, *Glomospira* sp., *Ammodiscus* cf. *incertus* (D'ORBIGNY), *Palaeolituonella* sp., *Miliolipora cuvillieri, Paleomiliolina* sp., *Dentalina* sp. and Oberhauserellidae sp.; Text-Fig. 14), and some fine unidentifiable bioclasts. The matrix is fractured, locally; the fractures are filled by limonite and calcite. A larger part of the lithoclasts derived from the subtidal C facies of the Dachstein Limestone, probably from the underlying bed. These are mm to cm sized clasts (Plate 4/1, 2). Peloidal, bioclastic grainstone is the most typical texture of these lithoclasts, some of them contain intraclasts, and recognisable foraminifera (mainly Involutinidae, like *Angulodiscus friedli, A. tenuis* and *Aulotortus sinuosus* and *Trochammina almtalensis* KOEHN-ZANINETTI, moreover *Diplotremina*? sp., *Agathammina austroalpina, Ophthalmidium* spp., *Pilammina densa, Planiinvoluta* cf. *deflexa* LEISCHNER, *Valvulina* sp. *Frondicularia woodwardi*) and radiolarians (Text-Fig. 14). Bioclastic wackestones also occur, sporadically. The clasts were commonly subject to micritization, microsparitization, and in some cases the original texture could not be recognised. The black pebbles are usually strongly micritized, their original textures have commonly disappeared in some patches or totally. Rarely the original depositional texture could be determined. In a 0.8 cm sized unrounded blackened grain the oolitic, peloidal, bioclastic texture was still visible (Plate 3/3), but it was overprinted by a dense network of filaments (Plate 4/4). Reddish, micritic pedogenically altered grains also occur.

Based on the presence of *Agathammina austroalpina*, and *Miliolipora cuvillieri* (KRISTAN-TOLLMANN, 1962; BRÖNNIMANN et al., 1972) and the lack of *Triasina hantkeni* suggest Norian, probably Late Norian age of the samples studied.

According to the above described phenomena, the typical history for the cycle ending subaerial exposure period can be summarised as follows. Subsequent to the emer-

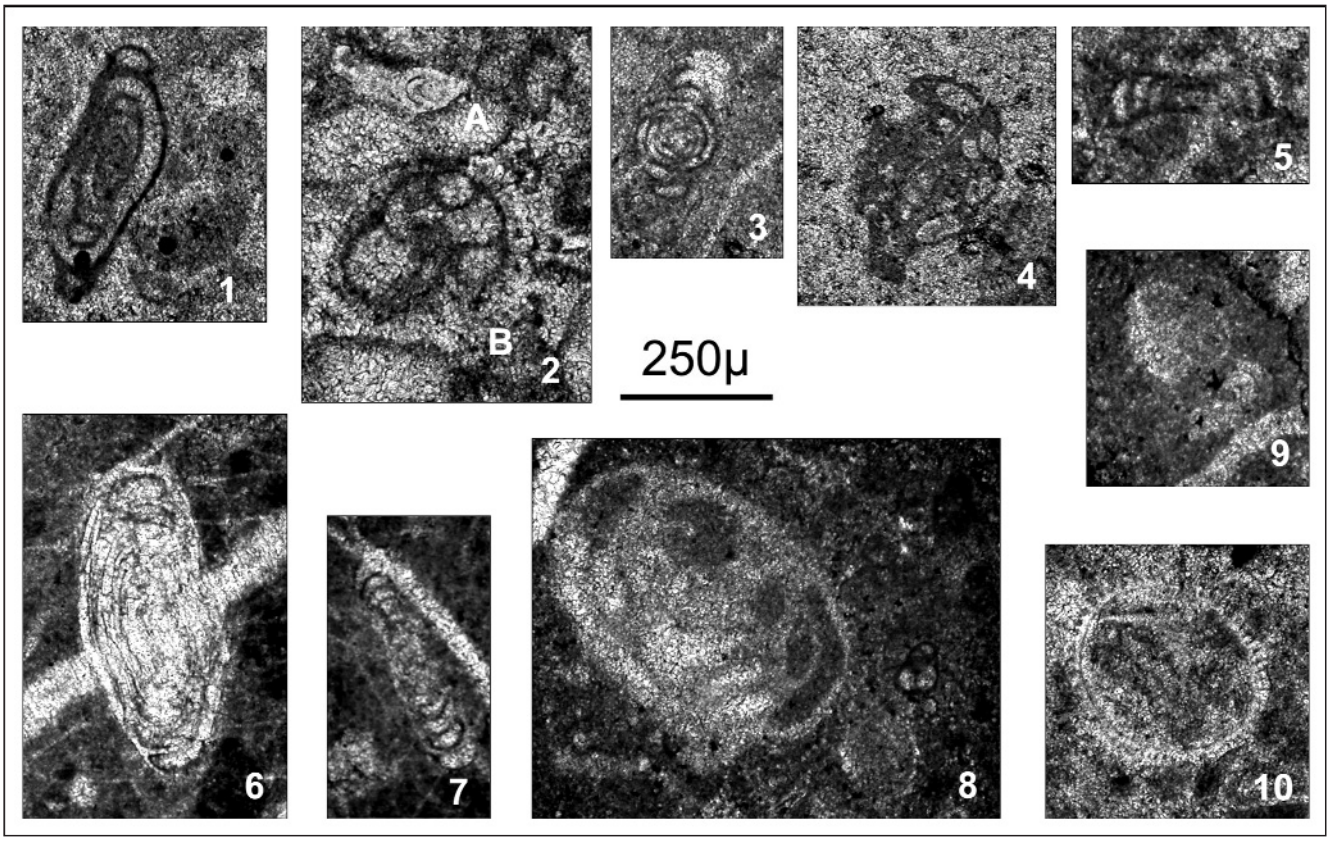

Text-Fig. 14.
Foraminifera of the section in the ski trail between Gjaidalm and Krippenstein.
1 = *Agathammina austroalpina* KRISTAN-TOLLMANN & TOLLMANN, sample G 2; 2 = *Frondicularia woodwardi* HOWCHIN (A) and *Trochammina almtalensis* KOEHN-ZANINETTI (B), sample G 2; 3 = *Glomospirella amplificata* KRISTAN-TOLLMANN, sample G 3; 4 = *Pilammina densa* PANTIČ, sample G 2; 5 = *Ammodiscus* cf. *incertus* (D'ORBIGNY), sample G 3; 6 = *Aulotortus sinuosus* WEYNSCHENK, sample G 3; 7 = *Angulodiscus tenuis* KRISTAN, sample G 3; 8 = *Angulodicus friedli* (KRISTAN-TOLLMANN), sample G 3; 9 = Oberhauserellidae sp., sample G 3; 10 = Radiolaria, sample G 3.

sion the physical, chemical and biological weathering of the previously deposited, semi-consolidated to consolidated carbonates may have been very intense leading to solution, karstification, and accordingly formation of an uneven surface, accumulation of debris of the underlying beds on it and development of cavities below the surface. These processes were supported by the appearance of the pioneer plants, and the onset of pedogenesis. Fragments of the pedogenically altered micritized, locally blackened carbonates also contributed to the clasts veneer formed on the karstic surface. Irregularly shaped intraclasts (soil clasts) and black pebbles are typical components of the tidal flat deposits (SHINN, 1983). The soil clasts were formed via combination of shrinkage phenomena and disruption by roots and burrower organisms and it is considered as an incipient stage of calcrete formation (SHINN, 1983). The blackening of carbonates took place usually in meteoric diagenetic, pedogenic environments where decomposed organic matter impregnated the pre-existing lacustrine or peritidal carbonate sediments in reducing, slightly alkaline diagenetic environment (STRASSER & DAVAUD, 1983; STRASSER, 1984).

The next stage was the extension of the permanently inundated pools on the tidal flat which may have been the herald of a subsequent transgression. Ostracode-bearing clayey mud deposited in the karstic depressions of the exposed surface and infiltrated into the subsurface solution cavities.

4. Conclusions

1) In the investigated Norian Dachstein Limestone succession of the Dachstein plateau the Lofer cycles are usually bounded by pronounced disconformities showing characteristic features of subaerial erosion, weathering and karstic solution on and below the paleosurfaces.
2) In some cases there are only subtle traces of the subaerial exposure, that has manifested itself in the more pronounced solution features, and meteoric diagenetic alterations below the bedding planes. In these cases the distinction of the cycles is poorly constrained, ambiguous. Accordingly proper identification of the facies stacking and distinction of the cycles need excellent exposure conditions and detailed microfacies investigations.
3) There are unambiguous traces of pedogenesis and meteoric diagenesis which affected the subtidal-peritidal carbonate deposits during the emersion periods. Calcretes forming on the top of the truncated bed sets are typical. Rip-up chips of calcretes, pebbles of blackened carbonates are also common. They occur in the basal lag deposits of the overlying cycles together with clasts of the previously consolidated underlying carbonates, some of them had been encrusted by Fe-oxide.
4) Establishment of more or less permanent fresh-water pools over large parts of the tidal-flat may be considered as a herald of the rising sea-level. The first, typically ostracode-bearing pool deposits appeared in the karstic depressions and cavities.
5) Evidences for subaerial exposures between the subtidal-peritidal deposits strongly support the allocyclic control of the Lofer cyclicity in the study area. However, the role of autocyclic processes which may have influenced the facies changes cannot be excluded.

Acknowledgements

The present work was carried out in the framework of the bilateral research program between the Geological Institute of Hungary and the Geological Survey of Austria. It was supported by the Hungarian Scientific Research Found (OTKA 68224, leader T. Budai).

Plate 1 Foraminifera of the Gretl-Rast section

Fig. 1: *Auloconus permodiscoides* OBERHAUSER. Bed 1.

Fig. 2: *Glomospira regularis* LIPINA. Bed 1.

Fig. 3: Duostominidae (*Diplotremina*? sp.). Bed 2.

Fig. 4: *Agathammina austroalpina* KRISTAN -TOLLMANN & TOLLMANN. Bed 3a.

Fig. 5: *Gaudryina triadica* KRISTAN-TOLLMANN. Bed 3b.

Fig. 6: *Angulodiscus communis* KRISTAN. Bed 3b.

Fig. 7: *Miliolipora cuvillieri* BRÖNNIMANN & ZANINETTI. Bed 3b.

Fig. 8: *Frondicularia woodwardi* HOWCHIN. Bed 3b.

Fig. 9: *Dentalina* sp. Bed 3b.

Fig. 10: *Earlandinita* sp. Bed 3b.

Fig. 11: *Earlandia* sp. Bed 3b.

Figs. 12,14: *Angulodiscus communis* KRISTAN. Bed 4.

Fig. 13: *Angulodiscus* cf. *tenuis* KRISTAN. Bed 4.

Figs. 15,17: *Angulodicus friedli* (KRISTAN-TOLLMANN). Bed 4.

Fig. 16: *Angulodiscus* cf. *minutus* (KOEHN-ZANINETTI). Bed 4.

Fig. 18: *Angulodiscus gaschei* KOEHN-ZANINETTI & BRÖNNIMANN. Bed 4.

Fig. 19: *Angulodiscus* cf. *communis* KRISTAN. Bed 4.

Fig. 20: *Galeanella panticae* ZANINETTI & BRÖNNIMANN. Bed 4.

Fig. 21: *Semiinvoluta* sp. and ostracodes. Bed 5.

Fig. 22: Oberhauserellidae sp. Bed 5.

Fig. 23: *Turrispirillina* sp. Bed 6.

Fig. 24: *Turrispirillina minima* PANTIČ. Bed 6.

Fig. 25: *Angulodicus friedli* (KRISTAN-TOLLMANN). Bed 6.

Fig. 26: *Aulotortus* cf. *sinuosus* WEYNSCHENK. Bed 6.

Fig. 27: *Diplotremina* sp. Bed 7.

Fig. 28: *Miliolipora cuvillieri* BRÖNNIMANN & ZANINETTI. Bed 7.

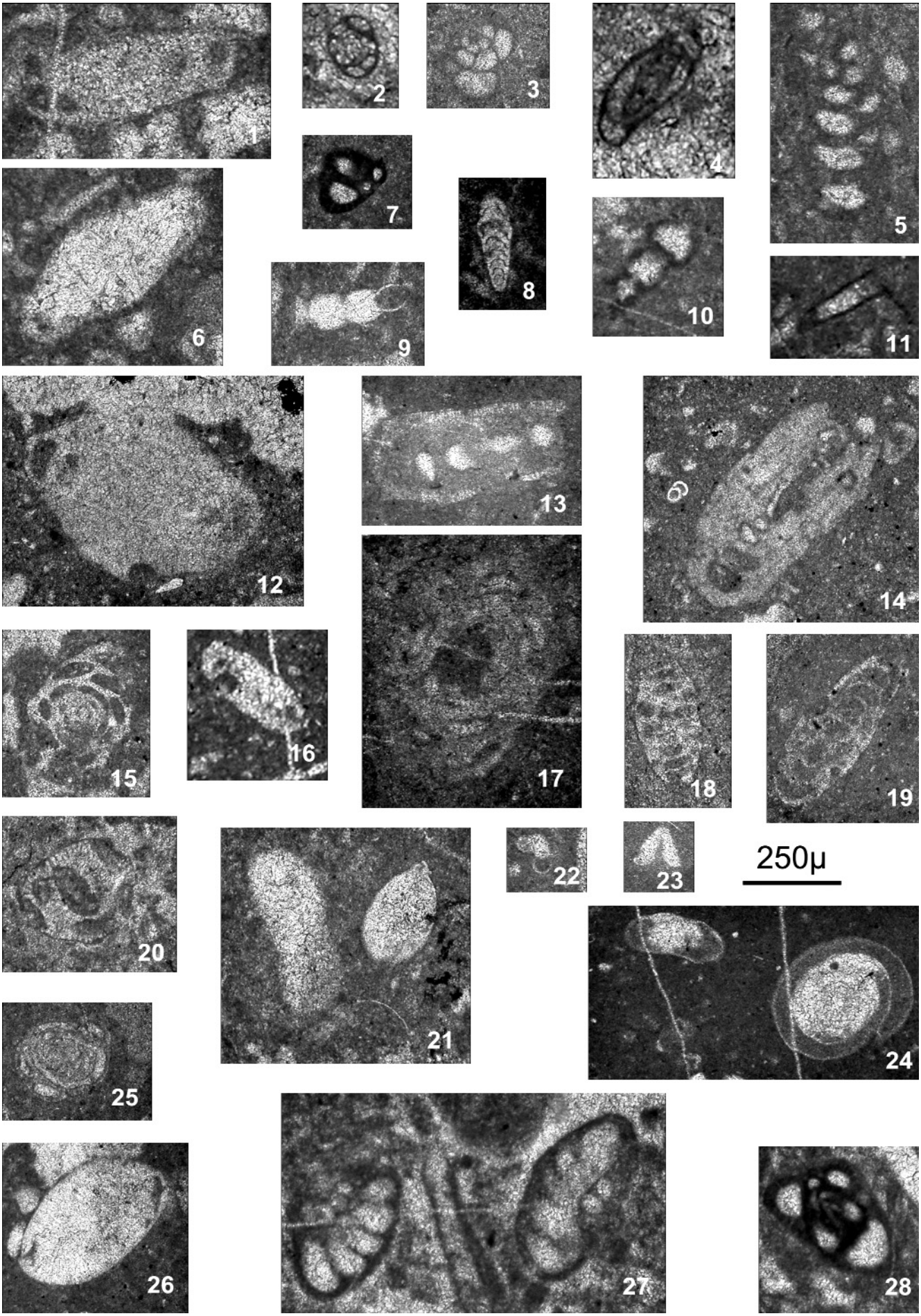
1
2
3
4
5
6
7
8
9
10
11
12
13
14
15
16
17
18
19
20
21
22
23
250µ
24
25
26
27
28

Plate 2

Fig. 1: Bioclastic wackestone with a network of solution pores filled by spar.
Bed 1, Gretl-Rast section.

Fig. 2: Solution cavity with geopetal fill.
There are thin-shelled ostracodes in the micritic sediment at the base of the cavity.
Bed 2, Gretl-Rast section.

Fig. 3: Peloidal packstone with bioclasts and biomolds and a larger intraclast.
Bed 3, Gretl-Rast section.

Fig. 4: Solution pore with geopetal fill.
Note the microbial crust formed probably on the upper wall of the cavity.
Bed 3, Gretl-Rast section.

Fig. 5: Wackestone with irregular and circum-granular cracks, indicating incipient pedogenesis.
Bed 4, Gretl-Rast section.

Fig. 6: Microsparite nodule in micritic matrix, and elongated solution cavities.
Bed 4, Gretl-Rast section.

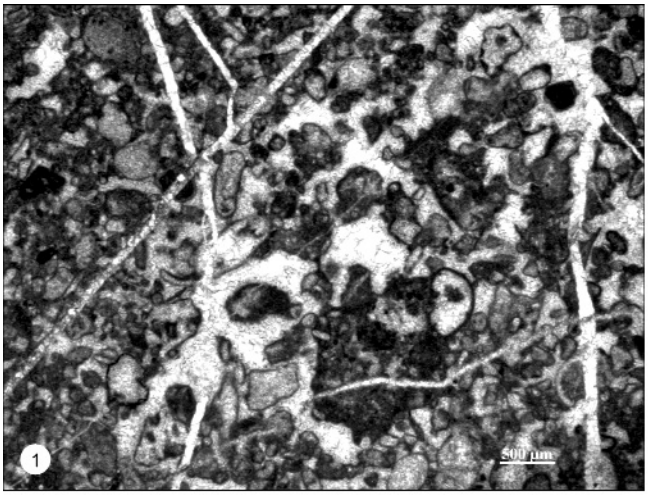
1
500 µm

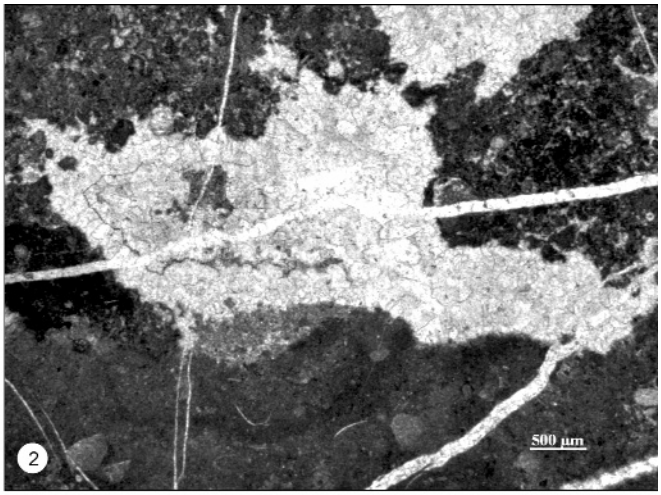
2
500 µm

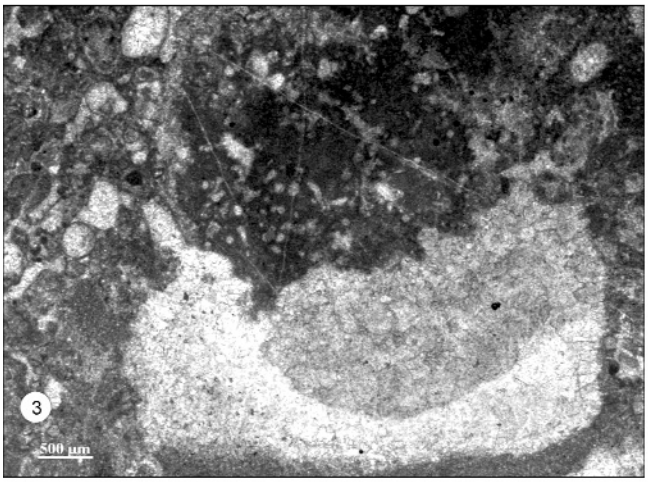
3
500 µm

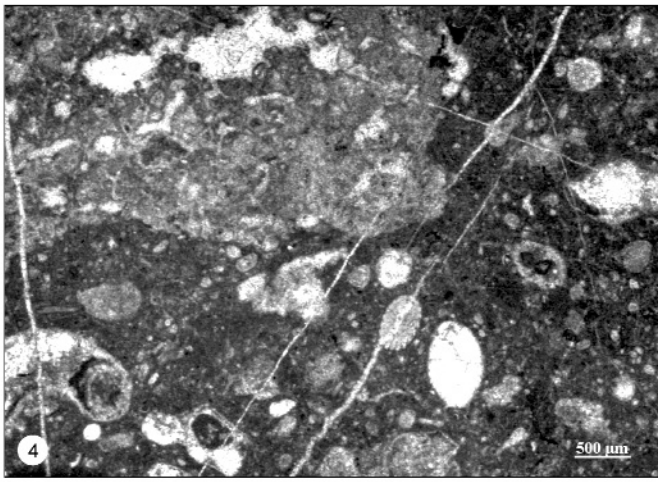
4
500 µm

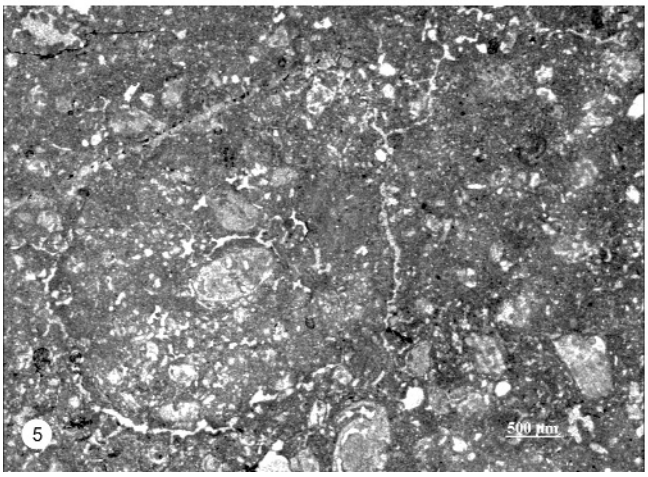
5
500 µm

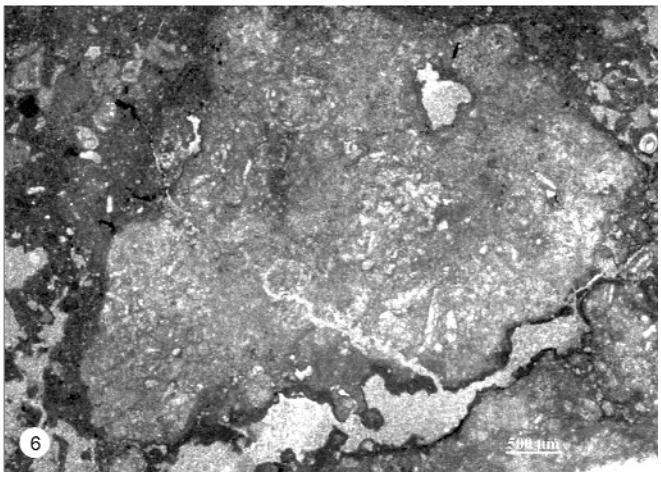
6
500 µm

Plate 3

Fig. 1: A dark lithoclast in bioclastic wackestone matrix.
Bed 4, Gretl-Rast section.

Fig. 2: Black mudstone clast with iron-oxyde coating.
Bed 4, Gretl-Rast section.

Fig. 3: Clotted peloidal microsparite abundant in thin-shelled ostracodes, in patches.
Bed 5, Gretl-Rast section.

Fig. 4: Elongated solution cavity with geopetal fill.
Bed 6, Gretl-Rast section.

Fig. 5: Solution pores filled by microsparite and sparite showing a circular structure; probably root cast.
Bed 6, Gretl-Rast section.

Fig. 6: Fragment of a chaetetid calcisponge.
Bed 7, Gretl-Rast section.

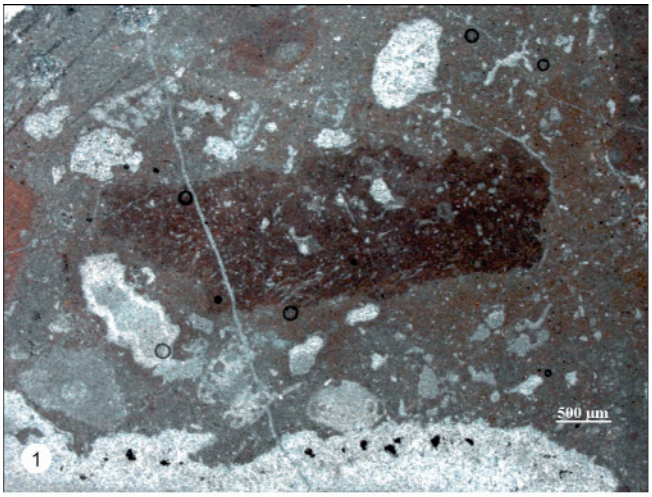
500 µm
1

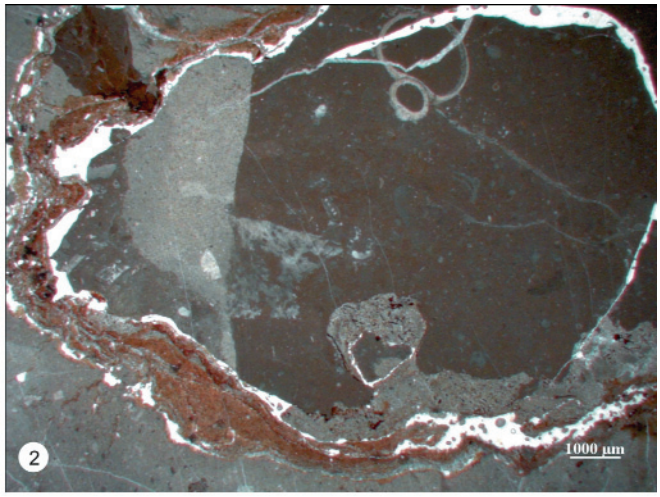
1000 µm
2

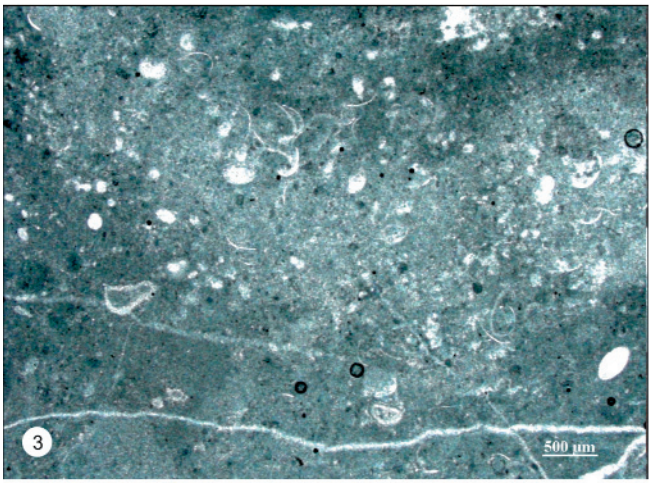
500 µm
3

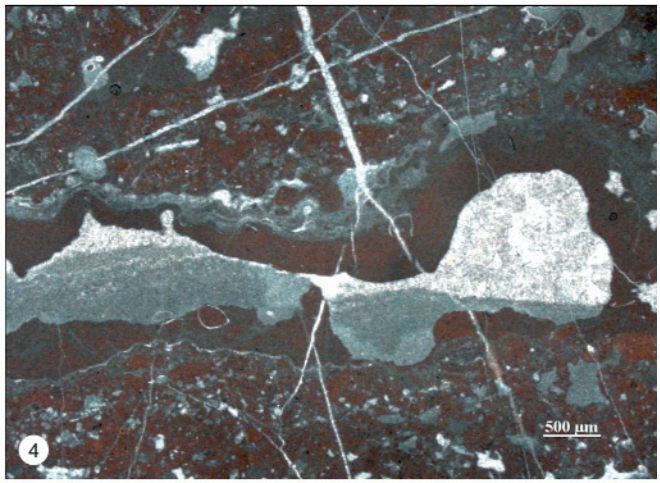
500 µm
4

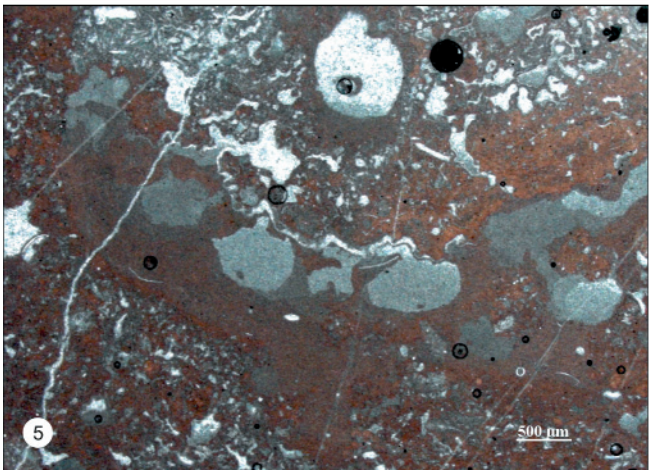
500 µm
5

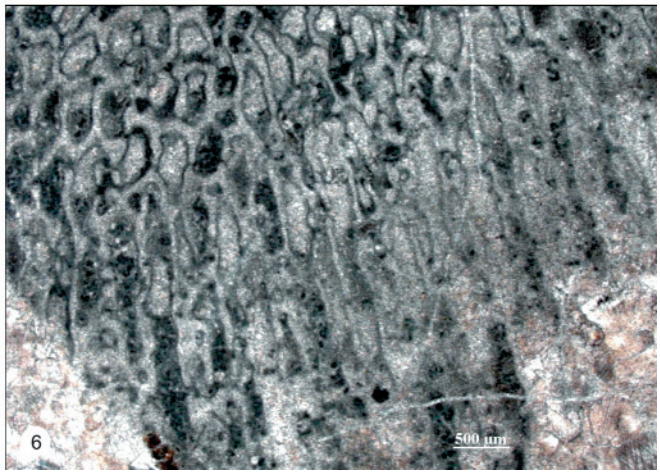
500 µm
6

Plate 4

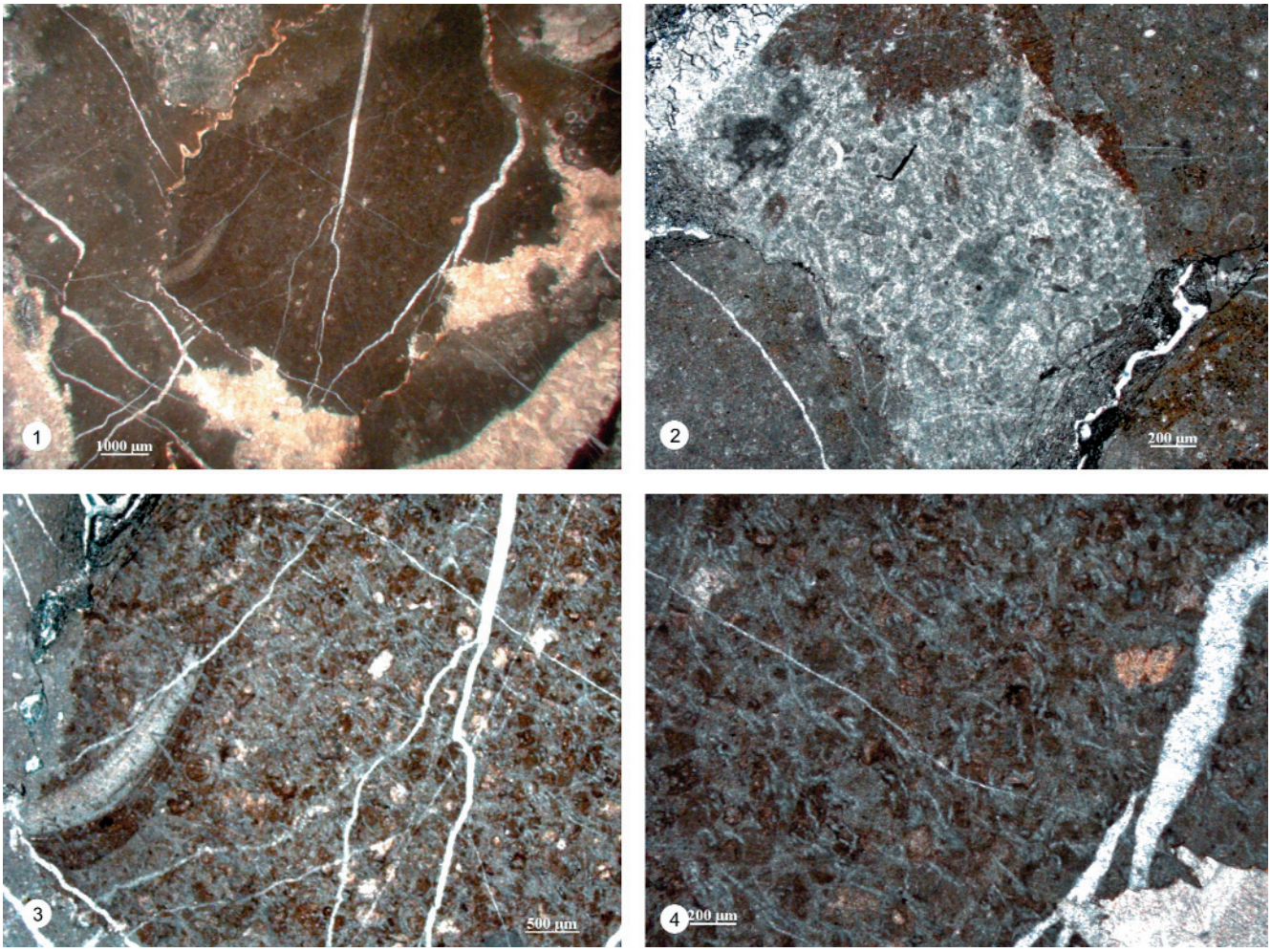

Fig. 1: Lithoclasts in mudstone-wackestone matrix, and solution vugs filled by sparry calcite.
Ski trail between Gjaidalm and Krippenstein (G 3).

Fig. 2: Peloidal grainstone lithoclast.
Ski trail between Gjaidalm and Krippenstein (G 3).

Fig. 3: Blackened clast with a bivalve shell fragment.
The originally ooidic, peloidal, bioclastic texture was subject to a strong alteration.
Ski trail between Gjaidalm and Krippenstein (G 3).

Fig. 4: A detailed image on the blackened and mictitized clasts shown on photo 3, a dense network of filaments is visible.

References

BRÖNNIMANN, P., ZANINETTI, L., BOZORGNIA, F., DASHTI, G.R. & MOSHTAGHIAN, A. (1972): Lithostratigraphy and Foraminifera of the Upper Triassic Naiband Formation, Iran. – Rev. de Micropal., **14** (5), 7–16.

ENOS, P. & SAMANKASSOU, E. (1998): Lofer cyclothems revisited (late Triassic, Northern Alps, Austria). – Facies, **38**, 207–228.

FISCHER, A.G. (1964): The Lofer cyclothems of the Alpine Triassic. – Kansas Geol. Surv. Bull., **169**, 107–149.

FLÜGEL, E. (1981): Paleoecology and facies of Upper Triassic Reefs in the Northern Calcareous Alps. – Soc. Econ. Paleont. Min. Spec. Publ., **30**, 291–359, Tulsa.

GOLDHAMMER, R.K., DUNN, P.A. & HARDIE, L.A. (1990): Depositional cycles, composite sea-level changes, cycle stacking patterns, and the hierarchy of stratigraphic forcing: Examples from Alpine Triassic platform carbonates. – Geol. Soc. Am. Bull., **102**, 535–562.

HAAS, J. (1982): Facies Analysis of the Cyclic Dachstein Limestone Formation (Upper Triassic) in the Bakony Mountains, Hungary. – Facies, **6**, 75–84.

HAAS, J. (1991): A basic model for Lofer Cycles. – In: EINSELE, G., RICKEN, W. & SEILACHER, A. (Eds.): Cycles and Events in Stratigraphy, Springer, New York, 722–732.

HAAS, J. (1994): Lofer cycles of the Upper Triassic Dachstein platform in the Transdanubian Mid-Mountains (Hungary). – Spec. Publ. Int. Ass. Sedim., **19**, Oxford, 303–322.

HAAS, J., LOBITZER, H. & MONOSTORI, M. (2007): Characteristics of the Lofer Cyclicity in the type locality of the Dachstein Limestone (Dachstein Plateau, Austria). – Facies, **53**, 113–126.

KOZUR, H. & ORAVECZ-SCHEFFER, A. (1972): Neue Ostracoden-Arten aus dem Rhät Ungarns. – Geol. Paläont. Mitt. Innsbruck, **2**, 1–14.

KRISTAN, E. (1957): Ophthalmiidae und Tetrataxinae (Foraminifera) aus dem Rhät der Hohen Wand in Nieder-Österreich. – Jb. Geol. B.-A., **100**, 269–298.

KRISTAN-TOLLMANN, E. (1962): Stratigraphisch wertvolle Foraminiferen aus Obertrias- und Liaskalken der voralpinen Fazies bei Wien. – Erdoel-Z., **78**, 228–233.

PANTIČ, S. (1967): *Turrispirillina minima* n. sp. from dinaric sediments of Triassic age. – Bull. Inst. Geol. Geoph. Res. Ser. A., **24–25** (1966/67), 255–258.

SANDER, B. (1936): Beiträge zur Kenntnis der Anlagerungsgefüge. – Mineral. und Petrogr. Mitteil., **48**, 27–139.

SATTERLEY, A.K. (1996a): Cyclic carbonate sedimentation in the Upper Triassic Dachstein Limestone, Austria: the role of patterns of sediment supply and tectonics in a platform-reef-basin system. – J. Sediment. Res., **66**(2), 307–323.

SATTERLEY, A.K. (1996b): The interpretation of cyclic succession of the Middle and Upper Triassic of the Northern and Southern Alps. – Earth. Sci. Rev., **40**, 181–207.

SCHWARZACHER, W. (1948): Über die sedimentäre Rhythmik des Dachsteinkalkes von Lofer. – Verh. Geol. B.-A., **1948**, 10–12, 175–188.

SCHWARZACHER, W. (1954): Die Grossrhythmik des Dachsteinkalkes von Lofer. – Tscherm. Miner. Petrogr. Mitt., **4**, 44–54.

SIMONY, F. (1847): Zweiter Winteraufenthalt auf dem Hallstätter Schneegebirge und drei Ersteigungen der hohen Dachsteinspitze (am 29. Jänner, 4. und 6. Februar 1847). – In: HAIDINGER, W. (Ed.): Berichte über die Mittheilungen von Freunden der Naturwiss. in Wien, **2**, 207–221.

SHINN, E. (1983): Tidal flat environment. – In: SCHOLLE, P.A., BEBOUT, D.G. & MOORE, C.H. (Eds.): Carbonate depositional environments, AAPG Memoir, **33**, 171–210.

SUESS, E. (1888): Das Antlitz der Erde. 2. Band. – Prag (F. Tempsky) – Wien (F. Tempsky) – Leipzig (G. Freytag).

STRASSER, A. (1984): Black-pebble occurrence and genesis in Holocene carbonate sediments (Florida Keys, Bahamas, and Tunisia). – Jour. Sed. Petrol., **54**/4, 1097–1109.

STRASSER, A. & DAVAUD, E. (1983): Black pebbles of the Purbackian (Swiss and French Jura): lithology, geochemistry and origin. – Eclogae Geol. Helv., **76**, 551–580.

WRIGHT, V.P. (1990): A micromorphological classification of fossil and recent calcic and petrocalcic microstructures. – In: DOUGLAS, L.A. (Ed.): Soil Micromorphology: A basic and Applied Science, Elsevier, Amsterdam, 401–407.

Manuskript bei der Schriftleitung eingelangt am 5. März 2009